

## Safety, dosimetry and tumor detection ability of $^{68}\text{Ga}$ -NOTA-AE105 - a novel radioligand for uPAR PET imaging: *first-in-humans study*

Dorthe Skovgaard<sup>1,2</sup>, Morten Persson<sup>2,3</sup>, Malene Brandt-Larsen<sup>1</sup>, Camilla Christensen<sup>1</sup>, Jacob Madsen<sup>1</sup>, Thomas Levin Klausen<sup>1</sup>, Søren Holm<sup>1</sup>, Flemming Littrup Andersen<sup>1</sup>, Annika Loft<sup>1</sup>, Anne Kiil Berthelsen<sup>1</sup>, Helle Pappot<sup>3</sup>, Klaus Brasso<sup>4</sup>, Niels Kroman<sup>5</sup>, Liselotte Højgaard<sup>1</sup>, Andreas Kjaer<sup>1\*</sup>

<sup>1</sup>Department of Clinical Physiology, Nuclear Medicine & PET and Cluster for Molecular Imaging, Rigshospitalet and University of Copenhagen, Copenhagen, Denmark

<sup>2</sup>Curasight, Copenhagen, Denmark

<sup>3</sup>Department of Oncology, Rigshospitalet, Copenhagen, Denmark.

<sup>4</sup>Copenhagen Prostate Cancer Center, Department of Urology, Abdominal Centre, Rigshospitalet, Copenhagen, Denmark.

<sup>5</sup>Department of Plastic Surgery, Breast Surgery and Burns Treatment, Rigshospitalet, Copenhagen, Denmark.

# These authors contributed equally to this work.

\*To whom correspondence should be addressed:

*Professor Andreas Kjaer, MD, PhD, DMSc*

*Department of Clinical Physiology, Nuclear Medicine & PET*

*KF-4012*

*Rigshospitalet, National University Hospital*

*Blegdamsvej 9*

*2100 Copenhagen*

*Denmark*

*E-mail: [akjaer@sund.ku.dk](mailto:akjaer@sund.ku.dk)*

**Short running title:** Phase I trial of  $^{68}\text{Ga}$ -NOTA-AE105 uPAR-PET

## **ABSTRACT**

Overexpression of urokinase-type plasminogen activator receptors (uPAR) represents an established biomarker for aggressiveness in most common malignant diseases, including breast (BC), prostate (PC) and urinary bladder cancer (UBC) and is therefore an important target for new cancer therapeutic and diagnostic strategies. In the study, uPAR Positron Emission Tomography (PET) imaging using a  $^{68}\text{Ga}$ -labelled version of the uPAR targeting peptide (AE105) was investigated in a group of patients with BC, PC and UBC. The aim of this first-in-humans, Phase I, clinical trial was to investigate safety and biodistribution in normal tissues and uptake in tumor lesions.

## **Methods**

Ten patients (6 PC, 2 BC and 2 UBC) received a single intravenous dose of  $^{68}\text{Ga}$ -NOTA-AE105 (154 + 59 MBq; range 48-208 MBq). The biodistribution and radiation dosimetry were assessed by serial whole body PET/CT scans (10 minutes, 1 and 2 hours p.i.). Safety assessment included measurements of vital signs with regular intervals during the imaging sessions and laboratory blood screening tests performed before and after injection. In a subgroup of patients, the *in vivo* stability of  $^{68}\text{Ga}$ -NOTA-AE105 was determined in collected blood and urine. PET images were visually analyzed for visible tumor uptake of  $^{68}\text{Ga}$ -NOTA-AE105 and Standardized Uptake Values (SUVs) were obtained from tumor lesions by manually drawing volumes of interest (VOIs) in the malignant tissue.

## **Results**

No adverse events or clinically detectable pharmacologic effects were found. The radioligand exhibited good *in vivo* stability and fast clearance from tissue compartments primarily by renal excretion. The effective dose was 0.015 mSv/MBq leading to a radiation burden of 3 mSv when using the clinical target dose of 200 MBq. In addition, radioligand accumulation was seen in primary tumor lesions as well as in metastases.

## **Conclusion**

This first-in-humans, Phase 1 clinical trial demonstrates the safe use and clinical potential of  $^{68}\text{Ga}$ -NOTA-AE105 as a new radioligand for uPAR PET imaging in cancer patients.

## INTRODUCTION

The urokinase-type plasminogen activator receptor (uPAR) is a cell membrane protein involved in extracellular matrix degradation. Besides regulating proteolysis, uPAR also activates many intracellular signaling pathways that promote cell motility, invasion, and proliferation through cooperation with transmembrane receptors. In normal tissues uPAR gene expression is limited. However, in cancer uPAR is frequently overexpressed, e.g. in urinary bladder cancer, uPAR immunoreactivity is detected in (96%) of the neoplasias at the invasive front [1] and in more than 500 breast cancer patients studied only 2% had uPAR levels below the detection limit [2]. Importantly, high uPAR expression is associated with cancer invasion and metastases. Accordingly, uPAR represents an established biomarker for aggressive disease and poor prognosis in a variety of human cancers, including the most common malignant diseases, such as breast (BC), colorectal, lung, urinary bladder (UBC) and prostate cancer (PC) [1, 3-11]. These observations highlight and support that non-invasive imaging of uPAR in cancer tissue could become a clinically relevant diagnostic and prognostic imaging biomarker with the possibility of distinguishing indolent tumors from the invasive phenotype.

Accordingly, we have for several years focused on development of radioligands based on the high affinity peptide antagonist AE105 for Positron Emission Tomography (PET) imaging of uPAR expression [12-17]. We recently published results from a promising *first-in-humans* study with  $^{64}\text{Cu}$ -DOTA-AE105 showing high uptake in both primary tumor lesions and lymph node metastases paralleled with high uPAR expression in excised tumor tissue, thereby providing evidence for uPAR PET imaging in cancer patients [4]. However, clinical translation of  $^{64}\text{Cu}$ -based radioligands is hampered by limited availability and the necessity of a cyclotron facility to produce the PET isotopes. In line with this, the generator-based PET isotope  $^{68}\text{Ga}$  has gained special attention because of its independence of an onsite cyclotron and a half-life of 68 min which matches well with the pharmacokinetics of peptides such as the AE105 [18]. The goal of the present phase I study was to investigate the feasibility of  $^{68}\text{Ga}$ -NOTA-AE105 for tumor imaging in humans. The primary aim was to evaluate the safety, pharmacokinetics and internal radiation dosimetry of a single-dose injection of the  $^{68}\text{Ga}$ -NOTA-AE105 in cancer patients using

PET/Computed Tomography (CT) imaging. The secondary objective was to investigate the uptake in primary tumor lesions and potentially in metastases if present.

## MATERIALS AND METHODS

### Study design

In this open-label phase I study, 10 patients with histopathologically confirmed PC (6 patients), BC (2 patients) or UBC (2 patients) were enrolled from May 2015 to July 2015 (Table 1). All patients gave written informed consent before inclusion. The study was approved by the Danish Health and Medicine Authority (EudraCT no 2014-005522-35) and the Ethical Committee of the Capital Region of Denmark (protocol H- 15002406). The study was registered in ClinicalTrials.gov (NCT02437539) and was performed in accordance with the recommendation for Good Clinical Practice including independent monitoring by the Good Clinical Practice unit of the Capital Region of Denmark. All patients were injected intravenously (i.v.) with approximately 200 MBq of <sup>68</sup>Ga-NOTA-AE105 followed by sequential whole-body PET/CT scans 10 minutes, 1 and 2 hours post injection (p.i.). The dose was chosen to provide adequate count statistics and was projected based on preclinical data to be well below the maximum acceptable radiation exposure and at the same level as an FDG-PET. In a subset of 6 patients (patient #4, #5, #6, #7, #8 and #10), blood was collected approximately 1, 5, 30 and 90 minutes p.i. for pharmacokinetic analysis, including ligand stability. Urine was collected from 3 patients (patient #7, #8 and #10) during the test period. Safety measures included observation and systematic questions of subjective well-being, monitoring of heart rate and blood pressure with regular intervals before, during and after the last image session (1 min 10 min, 1 h and 2 h p.i.). Hematological (Hb, WBC, platelets), liver (ALAT, AP, LDH) and renal function (s-creatinine, GFR, sodium, potassium) were measured before radioligand administration, immediately after and on return to the hospital 3-21 days following the study day (Supplemental Fig. 3). When available, preoperative biopsies or surgical excised primary tumor tissue and local lymph nodes were collected for target validation with immunohistochemical expression of uPAR.

## **Production of $^{68}\text{Ga}$ -NOTA-AE105**

NOTA-AE105 trifluoroacetate was obtained from ABX GmbH. Gallium-68 ( $t_{1/2} = 68$  min;  $E_{\max}, \beta^+ = 1.90$  MeV (89%)) labelling of NOTA-AE105 trifluoroacetate was performed using a Modular-Lab Standard module (Eckert & Ziegler). The  $^{68}\text{Ge}/^{68}\text{Ga}$  generator (IGG100, Eckert & Ziegler) was eluted with 6 ml 0.1M HCl. The eluate was concentrated on a Strata-XC cartridge and eluted with 700  $\mu\text{l}$  0.82M HCl/Acetone (2:98). NOTA-AE105 (32 nmol), dissolved in 10  $\mu\text{l}$  DMSO, was labelled in 500  $\mu\text{l}$  0.7M NaOAc buffer pH 5.2 and 200  $\mu\text{l}$  96 % EtOH at room temperature for 12 min. The resulting product,  $^{68}\text{Ga}$ -NOTA-AE105, was purified on a SepPak C18 light cartridge, eluted with 50 % ethanol, and formulated with saline to a total volume of 7 ml.

For analysis, a high-performance liquid chromatograph (HPLC) (Ultimate 3000; Dionex) was used with a 2.6  $\mu\text{m}$ , 100  $\text{\AA}$ , 50  $\times$  4.6 mm C18 column (Kinetex) and with the UV- and radiodetector connected in series. The mobile phases were: eluent A: 10% MeCN in  $\text{H}_2\text{O}$  with 0.1% trifluoroacetic acid; eluent B: 10%  $\text{H}_2\text{O}$  in MeCN with 0.1% trifluoroacetic acid. For thin layer chromatography (TLC) a ScanRam scanner and plates were used. The mobile phase was 77 g/L ammonium acetate in water/methanol (1:1). For gas chromatography (GC) a Shimadzu GC2014 was used with a Zebron ZB-WAX 30 m  $\times$  0.53 mm  $\times$  1.00  $\mu\text{m}$  column.

## **PET/CT acquisition**

All subjects fasted 6 hours prior to injection of  $^{68}\text{Ga}$ -NOTA-AE105. Two peripheral i.v. catheters were placed, one for radiotracer injection and one in the contra-lateral arm for withdrawal of blood samples and administration of CT contrast agent.

Data acquisition was performed using a PET/CT system (Biograph mCT, Siemens Medical Solutions, Erlangen, Germany) with an axial field of view of 216 mm. Emission scans were acquired 10 minutes, 1 and 2 hours following i.v. administration of  $^{68}\text{Ga}$ -NOTA-AE105 ( $\approx 200$  MBq). Whole-body PET scans were obtained in 3-dimensional mode, with an acquisition time of 2 minutes per bed position. Attenuation and scatter corrected PET data were reconstructed

iteratively using a 3D ordinary Poisson ordered-subset expectation-maximization algorithm including point spread function and time of flight information (Siemens Medical Solutions), the settings were: 2 iterations, 21 subsets, 2 mm Gaussian filter and a 400 x 400 matrix. Pixel size in the final reconstructed PET image was approximately 2 x 2 mm with a slice thickness of 2 mm. Due to artifact; “halo effect” on  $^{68}\text{Ga}$ -NOTA-AE105 PET in the tissue surrounding the urinary bladder caused by the prompt gamma of  $^{68}\text{Ga}$  at 1077 keV (branching ratio of 3.2%)[19], all image data were also reconstructed using prompt gamma correction. A diagnostic CT scan was obtained before the 1 hour PET scan, with a 2-mm slice thickness, 120 kV, and a quality reference of 225 mAs modulated by the Care Dose 4D automatic exposure control system (Siemens Medical Solutions). A low-dose CT scan, 2-mm slice thickness, 120 kV, and 40 mAs, was acquired before each of the 10 minutes and 2 hour scans and used for attenuation correction. An automatic injection system was used to administer 75 mL of an iodine containing contrast agent (Optiray 300; Covidien, Minneapolis, MN, USA) with a scan delay of 60 s and flow rate of 1.5 mL/s, followed by an injection of 100 mL of NaCl with a flow rate of 2.5 mL/s. PET images in units of Bq/mL were used for quantitative analysis of tissue radioactivity concentrations for dosimetry purposes and for calculation of standardized uptake values (SUV).

### **Plasma pharmacokinetics and urine metabolite analysis**

The blood and urine samples were analyzed on a Dionex UltiMate 3000 column-switching High Pressure Liquid Cromatograph system with a Posi-RAM Module 4 as previously described [4]. The mobile phase for the extraction step was 0.1 % TFA in H<sub>2</sub>O, while the analytical step was a gradient method with solvent A, 0.1% TFA in MeCN: H<sub>2</sub>O 10:90, and solvent B, 0.1% TFA in MeCN:H<sub>2</sub>O 90:10 , both with a flow of 1.5 ml/min. Gradient: 0-6 min (extraction), 6-7 min 0-10% B, 7-13 min 10-65% B, 13-14 min 65-10% B, 14-15 min 10% B.

### **Dosimetry**

Dosimetry was based on the decay-uncorrected image sets from the three time-points supplemented with sampled urine-data (three patients) as previously described [4]. Briefly,

cumulated activity for each patient and organ was determined by integration of time-activity curves based on an average of three spherical VOIs placed in all major organs defined on CT images using Mirada RTx (Mirada Medical, London, UK). Individual urine excretion data were fitted to mono-exponentials yielding the fraction of injected activity excreted and a biological half-life of the process. All data were entered into OLINDA/EXM software (Vanderbilt University, Nashville, TN, USA) to obtain corresponding estimates of organ-absorbed doses and effective dose. OLINDA's Voiding Bladder Model was used with fraction and half-life from the fitted urine data as input and an assumed bladder voiding interval of 1 hour.

### **Tumor uptake by visual image analysis and activity quantification**

All image data were analyzed by a team consisting of a highly experienced certified specialist in nuclear medicine and a highly experienced certified specialist in radiology for the presence of lesions suspicious of cancer. Semi quantitative analyzes of visually detectable tumor lesions were done by drawing spherical volumes of interest (VOIs). Due to low counts the image quality of the last scan (2 hours p.i.) was suboptimal for assessing tumor uptake and therefore SUVs were calculated only from the generated VOIs for the first two PET scans (10 minutes and 1 hour p.i.) and parameterized as SUVmean and SUVmax. In some cases the standard PET reconstruction showed a reduced signal ("halo effect") around the urinary bladder. The halo led to hampered tumor visualization and to underestimation of SUVs of both normal and tumor tissue. Therefore, all PET image data were reconstructed again using prompt gamma correction. The data were subsequently re-analyzed for tumor uptake by the same team of specialist with > three months between interpretations and the SUVs presented here were obtained from prompt gamma-corrected images.

### **Collection of Tissue Samples and Immunohistochemistry of uPAR Expression**

Surgical specimens of primary tumors and metastases were obtained from two BC patients undergoing surgical treatment subsequently to <sup>68</sup>Ga-NOTA-AE105 PET. The time interval between <sup>68</sup>Ga-NOTA-AE105 PET and surgery was five and two days, respectively. Four of the patients with locally advanced PC underwent lymphadenectomy prior to radiation therapy.

None of these patients had lymph node metastases based on CT findings. Prostate tumor specimens were available from the preoperative prostate biopsies only (expect from patient 5, where the initial biopsy was taken at a regional hospital and therefore not available). The specimens were placed in formalin. Sections were prepared with paraffin sections (2.5 µm thick) and a standard immunohistochemistry technique (avidin–biotin–peroxidase) was performed to visualize the immunostaining intensity and distribution of uPAR receptors as previously described using the monoclonal antibody R2 [4]. In addition, HE staining was performed. The sections were visually evaluated for visible uPAR positive staining and scored as either positive or negative.

## **Statistics**

Significance of differences in vital signs and blood tests were evaluated by using ANOVA. A p value of < 0.05 was considered statistically significant.

## **RESULTS**

### **Radiochemistry**

All preparations complied with the specifications. The specifications and results of the <sup>68</sup>Ga-NOTA-AE105 preparations are given in Supplemental Table 1.

### **Patient safety and dosimetry**

The administered mass of NOTA-AE105 was  $13.6 \pm 8.7 \mu\text{g}$  (range 4.4-34.7 µg). The mean administered activity was  $154 \pm 59 \text{ MBq}$  (range 48-208 MBq). None of the patients experienced infusion-related reactions or adverse events. There were no clinically detectable pharmacologically effects of <sup>68</sup>Ga-NOTA-AE105 and no changes in general well being or vital signs (supplementary 2). No acute or long-term effects on blood parameters and/or organ (liver and kidney) functions were found based on standard biochemical parameters before and after participation in this study (Supplemental Fig. 3). The dose calculations yielded an effective dose

of 0.015 mSv/MBq (Table 2). The bladder was the organ with the highest absorbed dose (0.131 mGy/MBq), followed by the kidneys (0.070 mGy/MBq).

### **Biodistribution, pharmacokinetics and image quality**

A characteristic imaging series, illustrating biodistribution at 10 minutes, 1 and 2 hours p.i., is shown in Figure 1. The excretion route appeared to be mainly through the kidneys with no or very little excretion through the hepatobiliary/gastrointestinal tract. Persistently, there was a relatively high, but decreasing blood pool activity and virtually no activity was found in the brain, lung, bone and muscle.

Six out of ten patients (patient #4, #5, #6, #7, #8 and #10) in the study were used for investigating the plasma pharmacokinetics of  $^{68}\text{Ga}$ -NOTA-AE105. A plasma half-life of 8.5 min was found. Only intact  $^{68}\text{Ga}$ -NOTA-AE105 and no major metabolites were detected in plasma or urine (Supplemental Table 4).

### **Tumor uptake of $^{68}\text{Ga}$ -NOTA-AE105 and ex vivo target validation**

The secondary objective of this study was to investigate the uptake of  $^{68}\text{Ga}$ -NOTA-AE105 in malignant tissue in BC, PC and UBC. Patient specific clinical information and imaging findings are detailed in Table 3.

#### **Breast cancer**

Two BC patients were included prior to surgical intervention (patient #1 and #6). On qualitative image analysis primary tumor uptake was clearly visualized already at the first (10 minutes) and at the 1 hour PET scan. In addition, the  $^{68}\text{Ga}$ -NOTA-AE105 PET scan clearly visualized metastatic spread to the ipsilateral axillary lymph nodes in both patients. This was confirmed with operative findings and final histopathological staging (Fig. 2). One of these patients (patient #6) was positive on the preoperative routine examination with ultrasound and fine needle biopsies, while in patient #1 the metastatic spread was found only during sentinel node

operation and the following complete axillary lymph node dissection confirmed metastatic spread to two out of 19 lymph nodes. uPAR immunohistochemistry on surgical specimens of primary tumors and metastatic lymph nodes in both patients, confirmed positive uPAR expression.

### **Prostate cancer**

Of the six patients with PC, four patients with newly diagnosed locally-advanced PC (patient #2, #3, #4 and #10) were included in the study prior to a planned open staging procedure with pelvic lymph node dissection. In these patients a low, heterogeneous intraprostatic distribution of the radioligand was found with no distinct tumor uptake and no detectable tracer uptake in regional lymph nodes. The latter was in line with the findings following staging as pathological examinations of the removed pelvic lymph nodes showed no lymph node involvement. The remaining two patients with PC (patient #7, #8) had bone metastases and were evaluated prior to chemotherapy. Both patients had multiple metastases with significant  $^{68}\text{Ga}$ -NOTA-AE105 uptake in several malignant lesions concurrent with heterogeneous uptake at the site of the primary tumor within the prostate gland. In the three available pre-operative prostate biopsies immunohistochemistry confirmed uPAR expression (Fig. 3).

### **Urinary bladder cancer**

Two patients with UBC were included in the study during an ongoing chemotherapy regime with only a small amount of residual disease. Both patients had proven response to chemotherapy, as evaluated by routine CT-scans, prior to inclusion in the present study. In one patient (patient #9) there was no visible uptake of  $^{68}\text{Ga}$ -NOTA-AE105 in 2 liver metastases, which was identified on the concomitant contrast-enhanced CT. No other lesions could be identified on neither  $^{68}\text{Ga}$ -NOTA-AE105 nor diagnostic CT with i.v. contrast.

## **DISCUSSION**

In this first-in-humans study we present the results of a  $^{68}\text{Ga}$ -labelled uPAR PET radioligand  $^{68}\text{Ga}$ -NOTA-AE105. Together with our previous phase I study with the  $^{64}\text{Cu}$ -labelled DOTA-

AE105, the present study confirms that it is possible to detect uPAR expression in tumor lesions *non-invasively* with PET/CT.

uPAR-PET/CT imaging with  $^{68}\text{Ga}$ -NOTA-AE105 was safe with no adverse events or obvious changes in general well-being or any vitals signs. In addition, no significant changes in total blood count, kidney or hepatic function occurred.

As expected, the biodistribution analysis revealed the primary excretion route to be renal with resulting high activity accumulation of  $^{68}\text{Ga}$ -NOTA-AE105 in kidneys and urinary bladder due to the high hydrophilicity and small size of the peptide. In addition, a relatively high blood pool activity could indicate some protein bound activity of the intact  $^{68}\text{Ga}$ -NOTA-AE105 or free  $^{68}\text{Ga}$  bound to transferrin [20]. The decreasing blood pool activity argues against continuous transchelation of  $^{68}\text{Ga}$  to transferrin and the radioligand cleared fast from organs and the blood pool activity probably reflects plasma protein bound activity. Compared to our  $^{64}\text{Cu}$ -DOTA-AE105, we found a lower accumulation of activity in the liver following injection of  $^{68}\text{Ga}$ -NOTA-AE105, which is favorable with respect to evaluation of possible liver metastases. Apart from the urinary tract, no other organ or tissues exhibited high non-specific uptake of  $^{68}\text{Ga}$ -NOTA-AE105.

The effective radiation dose was 0.0153 mSv/MBq, equaling 3.1 mSv at an injected activity of approximately 200 MBq which was applied in the present study. This is lower or comparable to the radiation dose received from a standard FDG-PET, where the effective dose is approximately 0.019 mSv/MBq, equal to 5.7 mSv at a standard dose of 300 MBq [21]. The administration of i.v. contrast agent for the 1 hour PET/CT scan could potentially result in a modest overestimation of SUVs in background organs. However, this is not expected to have any clinically significant effect on the calculated radiation dose, as based on our results from a previous study the average error in  $\text{SUV}_{\text{mean}}$  was found to be only 1.6% in background organs[22]. In addition, it could be argued that a high tumor uptake potentially alters biodistribution. However, as the tumor burden in the current study was relatively small (localized prostate cancer, primary breast cancer with no signs of spread and urinary bladder cancer with minimal residual disease). We therefore believe that tumor uptake had

no influence of the biodistribution and the final organ dosimetry.

Importantly, the radiation dose to bone marrow was below the recommended threshold value of 3 mSv [23] Therefore, the radiation burden of uPAR PET with <sup>68</sup>Ga-NOTA-AE105 is of no clinical concern and the effective dose is comparable to that of other clinically applied <sup>68</sup>Ga-based PET radioligands, such as <sup>68</sup>Ga-labelled PSMA [24] and <sup>68</sup>Ga-DOTATATE/DOTATOC [25].

Plasma pharmacokinetic and urine metabolite analysis revealed intact <sup>68</sup>Ga-NOTA-AE105 in blood and urine and no formation of isotopic labeled metabolites, which is also found in other radioligands [26, 27].

As a secondary objective of this phase I study, tumor detection, incl. SUVs and semiquantitative tumor uptake values were evaluated. The radioligand performed well in visual detection of metastatic tumor lesions, especially in BC, where metastatic disease in ipsilateral axillary lymph nodes was found even in a situation where the preoperative work-up with ultrasound, fine needle aspiration and contrast-enhanced CT failed to detect the metastases. This is a clear clinical example of one potential future application of uPAR PET, since this patient could have gone directly to axillary lymph node dissection following uPAR PET and circumventing the other procedures if a uPAR PET had been performed preoperatively. The current procedure with preoperative fine needle biopsy only finds approximately 1/3 of the patients with metastatic spread [28]. Therefore, uPAR PET imaging could potentially be a superior technology for this purpose, when focusing on the high and specific radioligand uptake in lymph node metastases found in the present study. However, a sufficiently powered, controlled clinical trial has to be performed to prove this hypothesis.

The failure of <sup>68</sup>Ga-NOTA-AE105 PET to detect two metastases in the liver in a patient with disseminated UBC (patient #9) might question the application of <sup>68</sup>Ga-NOTA-AE105 for disseminated UBC. However, other PET radioligands, e.g. <sup>18</sup>F-FLT and <sup>18</sup>F-Galacto-RGD have also been reported to have lower activity in malignant liver lesions compared to the relatively high physiological uptake in normal liver tissue [29, 30]. Another explanation could be downregulation of uPAR expression and tumor inactivation as a result of clinical response to

chemotherapy prior to inclusion in the study. However, future studies to further investigate this hypothesis are warranted.

In PC and BC, tracer uptake in malignant tissue was visible on uPAR PET scans at 10 minutes and 1 hour p.i.. The optimal administered dose of  $^{68}\text{Ga}$ -NOTA-AE105 and time for PET/CT scan following injection still needs to be established, but it is likely within the first 60 minutes, which is also the case for other peptide-based radioligands such as  $^{68}\text{Ga}$ -PSMA [24],  $^{68}\text{Ga}$ -DOTATATE/TOC [31] and RGD-peptides [32].

Histopathological examination of the surgical specimens from the primary BC tumors/metastasis and the three available preoperative primary PC biopsies demonstrated uPAR expression in all patients supporting target specific uptake of  $^{68}\text{Ga}$ -NOTA-AE105. Although the preoperative PC biopsies, compared to breast cancer tissue, showed only weak uPAR expression, the limited number of patient samples made it impossible to apply a robust quantitative scoring system and no attempt was done to correlate *ex vivo* expression of uPAR in the excised surgical specimens with image-derived semiquantitative tracer uptake. It is possible that the general pattern of low, heterogeneous uptake of  $^{68}\text{Ga}$ -NOTA-AE105 in prostatic tumors reflects weak tumor uPAR expression in these six PC patients that had either localized disease or were treated with radio-/chemotherapy. A significant correlation of uPAR expression based on immunohistochemistry and tumor uptake of the comparable radioligand  $^{64}\text{Cu}$ -DOTA-AE105 has previously been demonstrated in murine tumor models [12]. However, future prospective studies should ideally include a detailed and complete co-registration between imaging and subsequent cross-section pathology.

The artifact (“halo effect”) in form of reduced activity around the urinary bladder with high physiological activity uptake due to urinary excretion has been described using other  $^{68}\text{Ga}$ -based ligands, like  $^{68}\text{Ga}$ -PSMA [33] and  $^{68}\text{Ga}$ -DOTATOC[34]. However, this is of no major concern since it is easily removed by prompt gamma correction, which will be implemented in future standard reconstruction algorithms for  $^{68}\text{Ga}$ -PET (personal communication with Siemens).

In addition to BC staging, a promising application of a uPAR-based imaging agent may be in providing an imaging biomarker to determine the aggressiveness of a tumor, thereby giving prognostic information with possible therapeutic implications.

## **CONCLUSION**

This first in human clinical study demonstrates the feasibility and potential of using a  $^{68}\text{Ga}$ -labelled version of the AE105 peptide for uPAR targeted PET imaging. The administration of  $^{68}\text{Ga}$ -NOTA-AE105 was safe, well tolerated and provided satisfactory image contrast and identification of primary tumors and metastases. The most promising results were found in breast cancer with clear identification of metastatic axillary lymph nodes. Future phase II studies in larger patient populations with this indication will investigate the application and utility of uPAR PET in relevant clinical settings.

## **ACKNOWLEDGMENTS**

This work was supported by the John and Birthe Meyer Foundation, the Danish National Advanced Technology Foundation, the Research Foundation of Rigshospitalet, the Capital Region of Denmark, the Novo Nordisk Foundation, the Lundbeck Foundation, the A.P. Moeller Foundation, the Svend Andersen Foundation, the Arvid Nilsson Foundation, Innovation Fund Denmark and the Danish Council for independent research.

The authors would like to thank all patients and their families for participating in this study. In addition, we will thank our excellent staff (BD, SS, EA, MP) at the department for taking part in the conduction of the study.

## REFERENCES

1. Dohn, L.H., et al., *uPAR Expression Pattern in Patients with Urothelial Carcinoma of the Bladder--Possible Clinical Implications*. PLoS One, 2015. **10**(8): p. e0135824.
2. Grondahl-Hansen, J., et al., *Prognostic significance of the receptor for urokinase plasminogen activator in breast cancer*. Clin Cancer Res, 1995. **1**: p. 1079-1087.
3. Persson, M. and A. Kjaer, *Urokinase-type plasminogen activator receptor (uPAR) as a promising new imaging target: potential clinical applications*. Clin Physiol Funct Imaging, 2013. **33**(5): p. 329-37.
4. Persson, M., et al., *First-in-human uPAR PET: Imaging of Cancer Aggressiveness*. Theranostics, 2015. **5**(12): p. 1303-16.
5. Jacobsen, B. and M. Ploug, *The urokinase receptor and its structural homologue C4.4A in human cancer: expression, prognosis and pharmacological inhibition*. Curr Med Chem, 2008. **15**(25): p. 2559-73.
6. Dano, K., et al., *Plasminogen activation and cancer*. Thromb Haemost, 2005. **93**(4): p. 676-81.
7. Foekens, J.A., et al., *The urokinase system of plasminogen activation and prognosis in 2780 breast cancer patients*. Cancer Res, 2000. **60**(3): p. 636-43.
8. Riisbro, R., et al., *Prognostic significance of soluble urokinase plasminogen activator receptor in serum and cytosol of tumor tissue from patients with primary breast cancer*. Clin Cancer Res, 2002. **8**(5): p. 1132-41.
9. Dohn, L.H., et al., *Urokinase-type plasminogen activator receptor (uPAR) expression is associated with T-stage and survival in urothelial carcinoma of the bladder*. Urol Oncol, 2015. **33**(4): p. 165 e15-24.
10. Almasi, C.E., et al., *Prognostic and predictive value of intact and cleaved forms of the urokinase plasminogen activator receptor in metastatic prostate cancer*. Prostate, 2011. **71**(8): p. 899-907.
11. Almasi, C.E., et al., *Urokinase receptor forms in serum from non-small cell lung cancer patients: relation to prognosis*. Lung Cancer, 2011. **74**(3): p. 510-5.
12. Persson, M., et al., *Quantitative PET of human urokinase-type plasminogen activator receptor with 64Cu-DOTA-AE105: implications for visualizing cancer invasion*. J Nucl Med, 2012. **53**(1): p. 138-45.
13. Persson, M., et al., *(68)Ga-labeling and in vivo evaluation of a uPAR binding DOTA- and NODAGA-conjugated peptide for PET imaging of invasive cancers*. Nucl Med Biol, 2012. **39**(4): p. 560-9.
14. Persson, M., et al., *Improved PET imaging of uPAR expression using new (64)Cu-labeled cross-bridged peptide ligands: comparative in vitro and in vivo studies*. Theranostics, 2013. **3**(9): p. 618-32.
15. Persson, M., et al., *First (18)F-labeled ligand for PET imaging of uPAR: in vivo studies in human prostate cancer xenografts*. Nucl Med Biol, 2013. **40**(5): p. 618-24.
16. Persson, M., et al., *Dosimetry of 64Cu-DOTA-AE105, a PET tracer for uPAR imaging*. Nucl Med Biol, 2014. **41**(3): p. 290-5.
17. Persson, M., et al., *Urokinase-Type Plasminogen Activator Receptor as a Potential PET Biomarker in Glioblastoma*. J Nucl Med, 2016. **57**(2): p. 272-8.
18. Velikyan, I., *Prospective of (6)(8)Ga-radiopharmaceutical development*. Theranostics, 2013. **4**(1): p. 47-80.
19. Hong, L., et al., *Prompt Gamma Correction for Ga-68 PSMA PET IEEE MIC 2015*, Conference record., 2015.
20. Roesch, F. and P.J. Riss, *The renaissance of the Ge/Ga radionuclide generator initiates new developments in Ga radiopharmaceutical chemistry*. Curr Top Med Chem, 2010. **10**(16): p. 1633-68.
21. Deloar HM, F.T., Shidahara M, Nakamura T, Watabe H, Narita Y, Itoh M, Miyake M, Watanuki S., *Estimation of absorbed dose for 2-[F-18]fluoro-2-deoxy-D-glucose using whole-body positron emission tomography and magnetic resonance imaging*. Eur J Nucl Med, 1998. **Jun**(25(6)): p. 565-74.
22. Berthelsen, A.K., et al., *PET/CT with intravenous contrast can be used for PET attenuation correction in cancer patients*. Eur J Nucl Med Mol Imaging, 2005. **32**(10): p. 1167-75.
23. INTERNATIONAL ATOMIC ENERGY AGENCY VIENNA, *STRATEGIES FOR CLINICAL IMPLEMENTATION AND QUALITY MANAGEMENT OF PET TRACERS*. 2009.
24. Herrmann, K., et al., *Biodistribution and radiation dosimetry for a probe targeting prostate-specific membrane antigen for imaging and therapy*. J Nucl Med, 2015. **56**(6): p. 855-61.
25. Sandstrom, M., et al., *Comparative biodistribution and radiation dosimetry of 68Ga-DOTATOC and 68Ga-DOTATATE in patients with neuroendocrine tumors*. J Nucl Med, 2013. **54**(10): p. 1755-9.

26. Szabo, Z., et al., *Initial Evaluation of [(18)F]DCFPyL for Prostate-Specific Membrane Antigen (PSMA)-Targeted PET Imaging of Prostate Cancer*. Mol Imaging Biol, 2015. **17**(4): p. 565-74.
27. Hofmann, M., et al., *Biokinetics and imaging with the somatostatin receptor PET radioligand (68)Ga-DOTATOC: preliminary data*. Eur J Nucl Med, 2001. **28**(12): p. 1751-7.
28. Cools-Lartigue, J. and S. Meterissian, *Accuracy of axillary ultrasound in the diagnosis of nodal metastasis in invasive breast cancer: a review*. World J Surg, 2012. **36**(1): p. 46-54.
29. Beer, A.J., *PET imaging of avb3 expression in cancer patients*.
30. Barwick, T., et al., *Molecular PET and PET/CT imaging of tumour cell proliferation using F-18 fluoro-L-thymidine: a comprehensive evaluation*. Nucl Med Commun, 2009. **30**(12): p. 908-17.
31. Velikyan, I., et al., *Quantitative and qualitative intrapatient comparison of 68Ga-DOTATOC and 68Ga-DOTATATE: net uptake rate for accurate quantification*. J Nucl Med, 2014. **55**(2): p. 204-10.
32. Iagaru, A., et al., *(18)F-FPPRGD2 PET/CT: Pilot Phase Evaluation of Breast Cancer Patients*. Radiology, 2014. **273**(2): p. 549-59.
33. Afshar-Oromieh, A., et al., *Comparison of PET/CT and PET/MRI hybrid systems using a 68Ga-labelled PSMA ligand for the diagnosis of recurrent prostate cancer: initial experience*. Eur J Nucl Med Mol Imaging, 2014. **41**(5): p. 887-97.
34. Gaertner, F.C., et al., *Evaluation of Feasibility and Image Quality of 68Ga-DOTATOC Positron Emission Tomography/Magnetic Resonance in Comparison With Positron Emission Tomography/Computed Tomography in Patients With Neuroendocrine Tumors*. Invest. Radiol., 2013. **48**(5): p. 263-272.

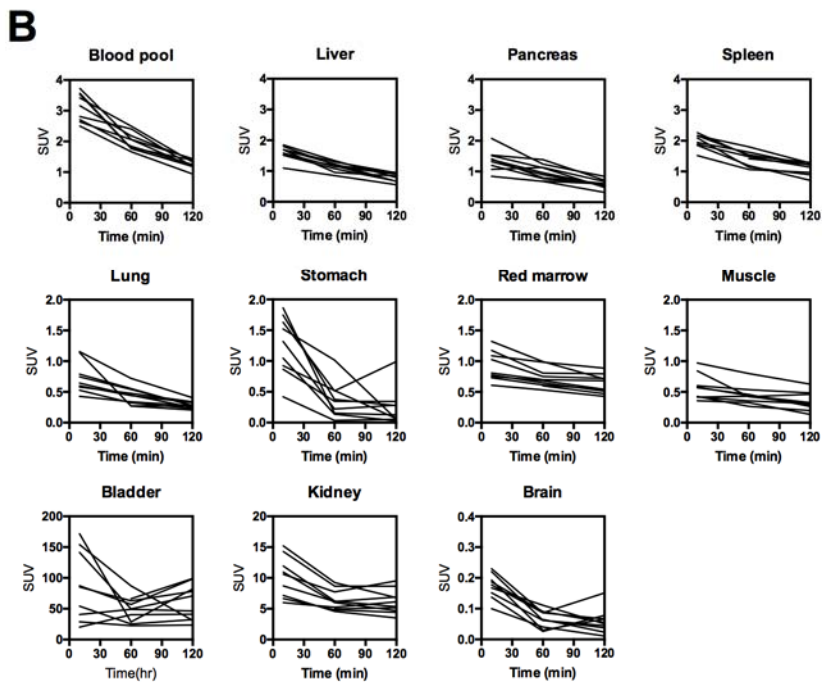
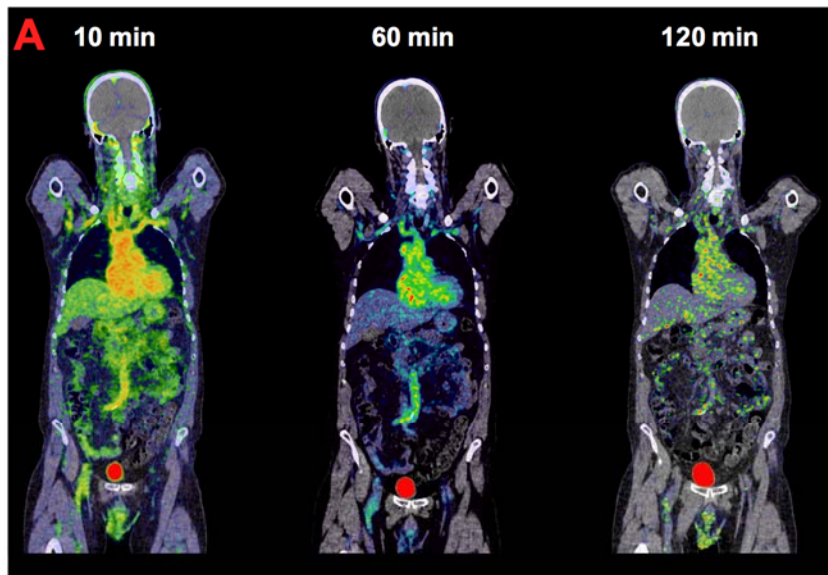


**Figure 1. Whole-body distribution and SUV in major organs following injection of  $^{68}\text{Ga}$ -NOTA-AE105.** (A) Maximum intensity projection PET images at 10 minutes, 1 and 2 hours following injection of  $^{68}\text{Ga}$ -NOTA-AE105 (patient 2). The highest accumulation of activity was in kidneys and bladder. (B) Decay corrected SUV values in blood and major organs plotted individually for  $n = 10$  patients. For each patient ROIs were drawn on selected organ of interest at all three consecutive PET scans.

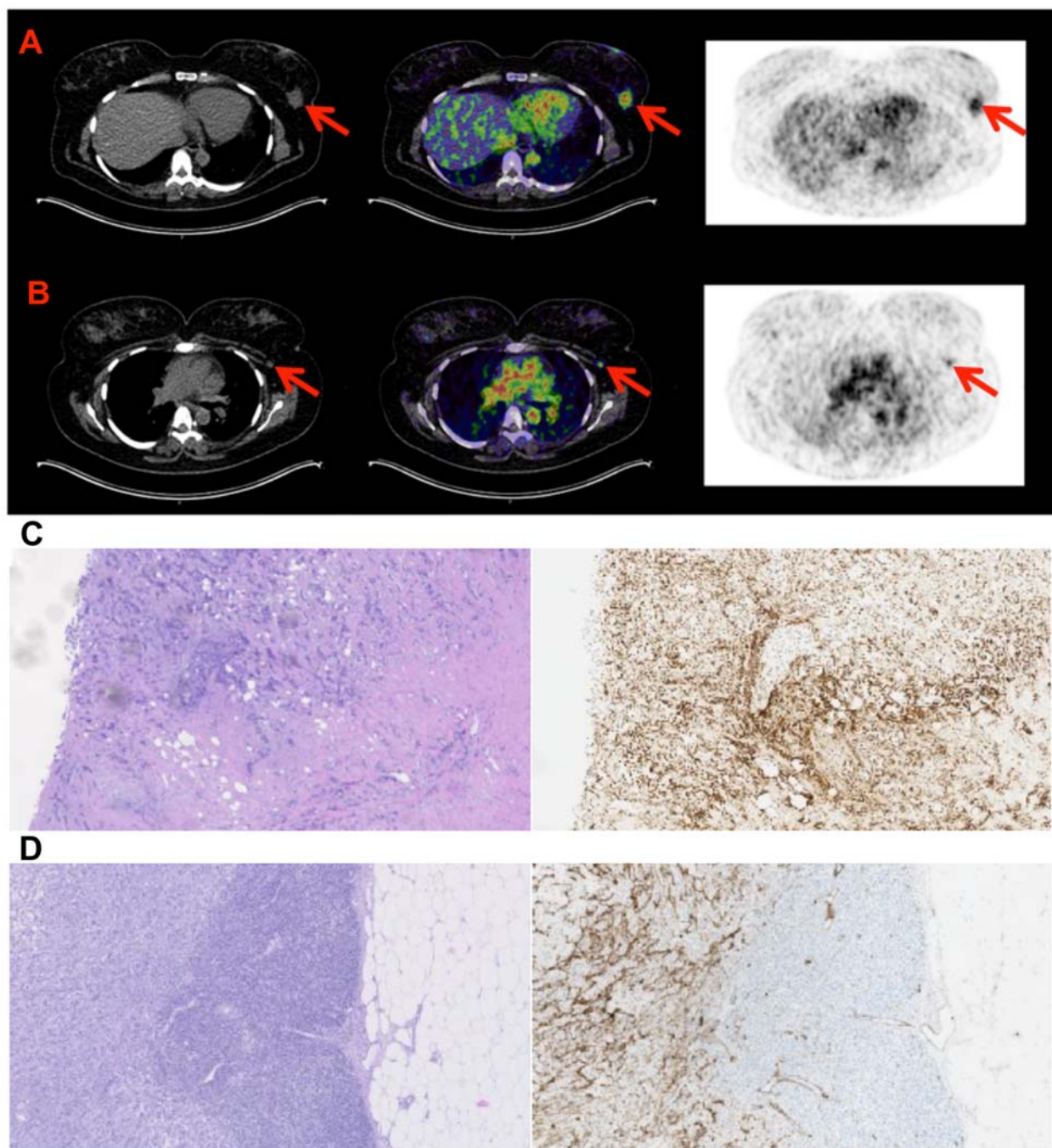


**Figure 2. uPAR PET imaging in breast cancer.** (A) Representative transverse CT, PET and co-registered PET/CT images of a primary tumor lesion with intense uptake of  $^{68}\text{Ga}$ -NOTA-AE105 (patient 1). (B) Images show a uPAR positive axillary lymph node metastasis (red arrow) with significant uptake in the same patient. (C) Representative slides with intense uPAR immunohistochemistry staining and corresponding HE staining of tumor tissue from the patient's primary tumor. (D) uPAR immunohistochemistry staining and corresponding HE staining of lymph node metastases.

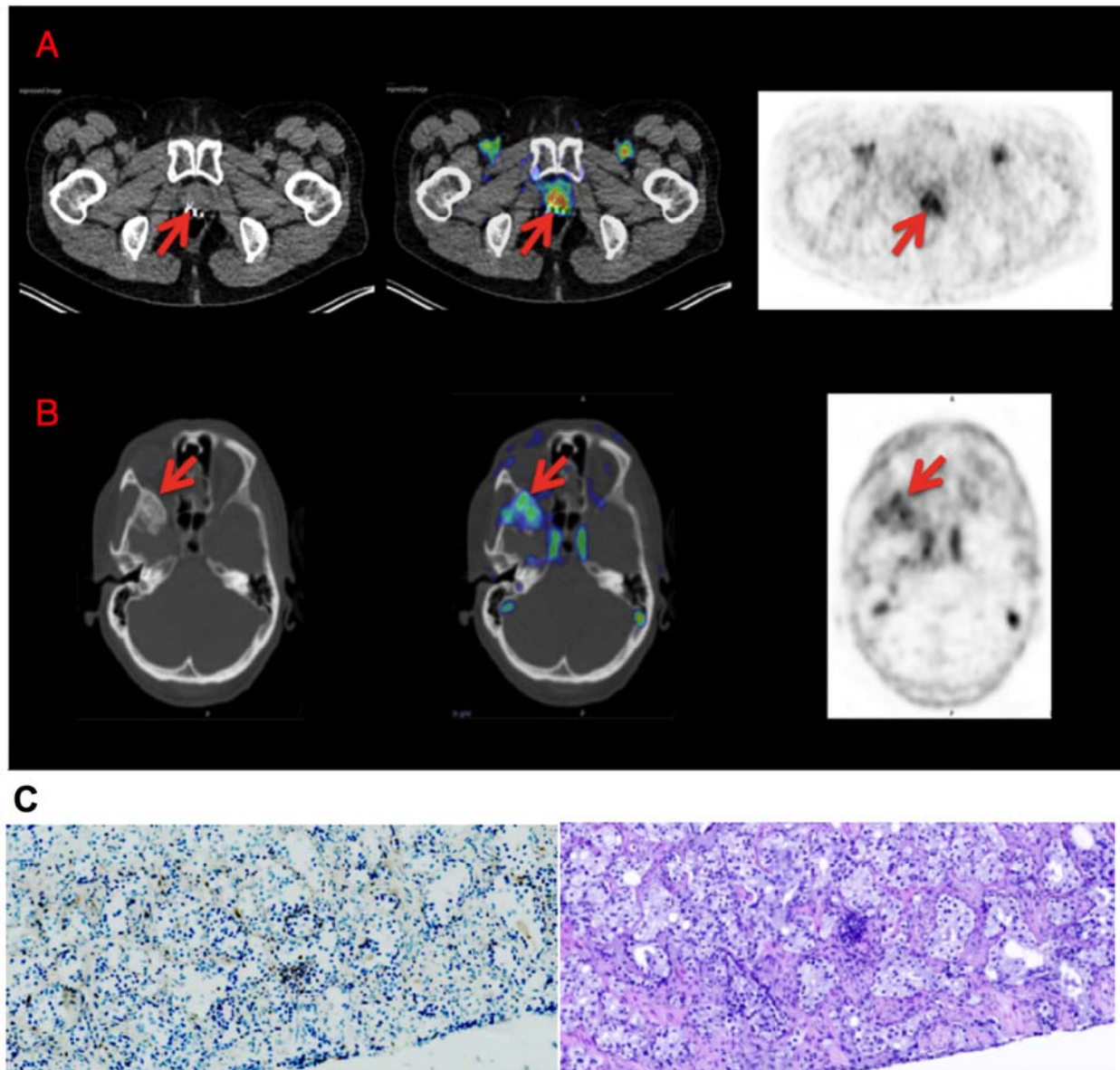


**Figure 3. uPAR PET imaging in prostate cancer.** (A) Representative transverse CT, PET and co-registered PET/CT images with uptake of  $^{68}\text{Ga}$ -NOTA-AE105 at the site of the primary tumor (patient 7). (B) Images show a uPAR positive metastasis in the sphenoid bone (red arrow) with significant uptake in the same patient. (C) Representative slides with weak uPAR immunohistochemistry staining of tumor tissue from a preoperative biopsy and corresponding HE staining (patient 10).

Patient	1	2	3	4	5	6	7	8	9	10
Gender	Female	Male	Male	Male	Female	Male	Male	Male	Male	Male
Age	51	70	74	67	28	71	57	52	66	74
Cancer type	Breast Ductal carcinoma	Prostate	Prostate	Prostate	Breast Ductal carcinoma	Bladder	Prostate	Prostate	Bladder	Prostate
Stage/Grade	Grade III	cT3N0M0	cT3N0M0	cT3N0M0	Grade II	Dissiminated disease - no residual lesions on treatment evaluation CT	Dissiminated bone metastases Initially treated with local radiotherapy (2008)	Dissiminated bone metastases at the time of diagnosis (2014)	Dissiminated disease - 2 liver metastases on treatment evaluation CT	cT3N0M0
Biomarker status	Estrogen positive HER-2 negative	Gleason score 4+5 PSA 56	Gleason score 4+5 PSA 23	Gleason score 3+4 PSA 9	Estrogen positive HER-2 positive	n.a.	PSA 128	PSA 11	n.a.	Gleason 4+5 PSA 8
Ongoing systemic therapies	No	No	No	No	No	Cisplatin & Gemzar (6 series)	Docetaxel (7 series)	Firmagon + Xgeva Docetaxel (6 series)	Cisplatin & Gemzar (6 series)	No
# days following PET scan before operation	5	9	2	14	2	n.a.	n.a.	n.a.	n.a.	20

**Table 1. Patient characteristics**

**Table 2 - uPAR Positron emission tomography dosimetry**

Organ/Tissue	Mean absorbed dose (mGy/MBq)
Adrenals	0.0118
Brain	0.00193
Breast	0.00599
Gallbladder wall	0.00838
Lower large intestine wall	0.00895
Small intestine	0.0177
Stomach wall	0.0114
Upper large intestine wall	0.0129
Heart wall	0.021
Kidneys	0.0699
Liver	0.0134
Lungs	0.00662
Muscle	0.00669
Ovaries	0.00909
Pancreas	0.012
Red marrow	0.00869
Osteogenic cells	0.0137
Skin	0.00564
Spleen	0.0146
Testes	0.00736
Thymus	0.00677
Thyroid	0.0128
Urinary bladder wall	0.131
Uterus	0.0109
Total body	0.00924
Effective dose (mSv/MBq)	<b>0.0153</b>

**Table 2. Dosimetry.** Mean absorbed dose per unit administrated (mGy/MBq) of major organs were derived from serial whole-body PET scans acquired 10 minutes, 1 and 2 hours following injection of  $^{68}\text{Ga}$ -NOTA-AE105 using VOI-based time activity data.

Table 3. Summary of uPAR PET/CT results and clinical workup

Patient #	uPAR PET	Primary tumor detection		10 minutes SUVmean	10 minutes SUVmax	1 hour SUVmean	1 hour SUVmax	uPAR immunohisto
		Routine clinical CT/Operation/biopsy						
1	breast	Breast cancer in biopsy and confirmed postoperatively		2.72	5.03	1.76	2.85	Positive
2	prostate	Prostate cancer in 12/12 biopsies		2.51	4.40	1.98	3.53	Positive
3	prostate	Prostate cancer in 12/12 biopsies		2.98	5.05	2.56	4.9	Positive
4	prostate	Prostate cancer in 12/12 biopsies		2.20	3.82	2.07	3.87	na
5	breast	Breast cancer in biopsy and confirmed postoperatively		2.52	3.83	2.26	3.86	Positive
6	0 urinary bladder lesions	No primary tumor on routine CT		na	na	na	na	na
7	prostate	Prostate cancer 11/12 biopsies (2008)		2.26	4.63	1.32	2.52	na
8	prostate	No biopsies from primary tumor/no routine CT/operation		1.82	3.74	1.23	2.69	na
9	0 urinary bladder lesions	No primary tumor on routine CT		na	na	na	na	na
10	prostate	Prostate cancer in 5/9 biopsies		2.22	4.76	0.69	2.20	Positive

		Metastases detection					
Patient #	uPAR PET	Routine clinical CT/Operation/biopsy	10 minutes SUVmean	10 minutes SUVmax	1 hour SUVmean	1 hour SUVmax	uPAR histology
1	2 axillary lymph node metastases	2 axillary lymph node metastases	2.56	3.41	1.53	2.08	Positive
2	No metastases	No lymph node metastases during staging operation	na	na	na	na	na
3	No metastases	No lymph node metastases during staging operation	na	na	na	na	na
4	No metastases	No lymph node metastases during staging operation	na	na	na	na	na
5	2 axillary lymph node metastases	2 axillary lymph node metastases	2.10	2.75	1.09	2.71	Positive
6	no lesions	No residual disease on routine CT	na	na	na	na	na
7	3 bone lesions	3 bone lesions on routine CT	1.86*	2.97*	1.22*	2.26*	na
8	Multiple bone lesions	Multiple bone metastases on routine CT	3.60*	4.88*	1.71*	2.36*	na
9	No uptake in 2 liver lesions	2 liver metastases on routine CT	na	na	na	na	na
10	No metastases	No lymph node metastases during staging operation	na	na	na	na	na

\* evaluation on 1 representative bone metastases

All primary prostate cancers showed heterogenous physiological tracer distribution and the SUVs are based on VOIs drawn using either CT tumor deliniation or whole prostate gland

**Table 3. Summary of uPAR PET/CT and immunohistochemistry of uPAR expression in available tumor tissue.**